Characterization of commercial supercapacitors for low temperature applications

E. Iwama [a,b], P.L. Taberna [a,b], P. Azais [c,1], L. Brégeon [c], P. Simon [a,b,*]

[a] Université Paul Sabatier de Toulouse, CIRIMAT, UMR-CNRS 5085, 31062 Toulouse, Cedex 9, France
[b] Réseau sur le Stockage Electrochimique de l'Energie, (RS2E) FR CNRS n°3459, France
[c] Batscap, Groupe BOLLORE, Odet-Ergué-Gabéric, 29556 Quimper, Cedex 9, France

HIGHLIGHTS

► Low temperature electrolytes were tested with commercial 600F SC cell.
► Mixing MA enlarged low temperature limit of AN-based SC cell from −40 to −55 °C.
► High temperature performance was exemplified by floating at 2.7 V and +60 °C.

ARTICLE INFO

ABSTRACT

Electrochemical characterizations at low temperature and floating tests have been performed on 600F commercial supercapacitor (SC) for acetonitrile (AN)-based and AN + methyl acetate (MA) mixed electrolytes. From −40 to +20 °C, AN electrolyte showed slightly higher capacitance than those of AN + MA mixed electrolytes (25 and 33 vol.% of MA). At −55 °C, however, AN electrolyte did not cycle at all, while MA mixed electrolyte normally cycled with a slight decrease in their capacitance. From electrochemical impedance spectroscopy measurements, the whole resistance for AN-based cells at −55 °C was found to be about 10,000 times higher than that of +20 °C, while a 40-fold increase in the cell resistance was obtained for the MA mixture between 20 and −55 °C. From the results of floating tests at 2.7 V and 60 °C for 1 month, the 25 vol.% MA mixture showed no change and slight decreased but stable capacitance.

1. Introduction

The increasing importance of global environment deterioration and diminishing energy supplies are major factors prompting the introduction of electrical energy devices into transportations such as vehicles, trains, and airplanes. In aeronautics for these days, apart from driving energy of airplanes, other energy supplies such as for navigation, a landing and a wing operation, lightning, and air conditioning during their flight become more and more indispensable. These auxiliary energy supplies depend on three energy systems, hydraulic, pneumatic, and electric. Recent investigations have been focused on replacing the former two systems with the electric system due to its advantages of i) less fuel depending, ii) smaller maintenance cost, iii) simpler design, and iv) less contamination in environment [1,2]. For the aeronautics applications (more electric aircraft; MEA), however, the required condition for the equipment is severe, especially for the energy device, which should be required to i) lightness of the device, ii) high power density iii) good cycleability, iv) credibility, and v) wide temperature range [2,3].

Supercapacitors (SCs), also called as ultracapacitors or electrochemical capacitors, are energy devices, which store electric charges in an electrical double layer at carbon electrode–electrolyte interface [4]. These devices provide higher power density (10^3–10^4 W kg^{-1}), medium energy density (≈ 5 Wh kg^{-1}), excellent cycleability (up to several millions), and relatively wider operational temperature range ($-40 < T < +70$ °C) [5], compared to batteries based on slow and temperature depending electrochemical reactions. Thanks to these safe and reliable properties, SC cells have been used for consumer electronics, memory back-up systems, industrial power and energy management, hybrid cars, catenary-free light

* Corresponding author. Université Paul Sabatier de Toulouse, CIRIMAT, UMR-CNRS 5085, 31062 Toulouse, Cedex 9, France. Tel.: +33 561556802; fax: +33 561556163.
    E-mail addresses: laurent.bregeon@batscap.com (L. Brégeon), simon@chimie.ups-tlse.fr (P. Simon).
[1] Present address: CEA-LITEN, 17 rue des Martyrs, 38054 Grenoble, Cedex 9, France.

rail vehicles and even aeronautics such as emergency opening doors on the Airbus A380 [6–10]. These reliable SC cells would be installed more and more into the MEA industry in the near future.

Generally, SC cells compose of two porous carbon electrodes attached on Al current collector and separated by porous membrane impregnated with an aqueous or nonaqueous electrolyte. From the viewpoint of energy density, nonaqueous electrolytes which consist of tetraethylammonium tetrafluoroborate (TEABF$_4$) with acetonitrile (AN) or propylene carbonate (PC) is preferred to aqueous electrolyte, due to their wider voltage window. Conventional SCs using AN, however, have faced a critical problem due to the high melting point of AN (-45 °C), considering the required operation temperature for MEA application is at -55 °C. Using PC instead of AN leads much limitation of the use in low temperature (>-25 °C) due to its lower ionic conductivity [3,11]. To overcome this low temperature issue, several investigations have been reported [3,12–17]. A. Jänes et al. firstly used the binary, ternary and quaternary mixture of ethylene carbonates and organic esters such as methyl acetate (MA), methyl formate (MF), and ethyl acetate (EA) for SC cells, and the certain mixtures showed the improved conductivity at low temperature than that of PC [12,13]. E.J. Brandon et al. reported SC performances at low temperature, using AN mixed with EA, MA, MF, or 1,3-dioxolane [3,14]. These co-solvents were chosen because of their low melting points, relatively low viscosity, and medium dielectric constants. Using triethylmethylammonium tetrafluorborate (TEMABFA$_4$) or spiro-(1,1')-bipyrrodium tetrafluoroborate (SBPBF$_4$) in AN and MF mixture solvents was also investigated [15,16]. Eutectic mixture of ionic liquids with exohedral carbons was recently reported as well [17]. These mixture electrolytes certainly showed promising characteristic enabling SC performance below the limit of temperature of AN -45 °C.

In this study, we chose MA as a co-solvent of AN, because of its low melting temperature of -98.0 °C and low viscosity of 0.364 cP (Table 1). These electrolyte mixtures have been used in commercial 600 F 12 W SC cells manufactured by Batscap. Low temperature charge-discharge down to -55 °C and the aging tests up to 60 °C were achieved to check the interest of these electrolytes for MEA applications.

2. Experimental

The low temperature measurements have been performed on a Batscap SC composed of activated carbon electrodes and an organic electrolyte with a nominal capacitance of 600 F, for temperatures between -55 and $+20$ °C. Tetraethylanmonium fluoroborate (TEABF$_4$, Acros Organics, 99%) was chosen as the electrolytic salt. Solvents used were acetonitrile (AN, Acros Organics, 99+%, extra dry < 50 ppm of water) and mixtures of AN and methyl acetate (MA, Alfa Aesar, 99%). Prepared electrolyte compositions were 1 M TEABF$_4$ in pure AN, AN + MA (75:25 in volume), and

AN + MA (67: 33). Electrolyte formulations were made in an argon-filled globe box (Braun, Unilab < 0.1 ppm of water and oxygen). Conductivity of the three electrolytes at different temperatures was measured by Zahner impedancemeter, in a two-electrodes Swagelok cell configuration. Each cell was composed of two stainless steel electrodes ($\phi = 1.1$ cm) and glass fiber separator ($\phi = 1.2$ cm, Whatman GF/B). Batscap assembled commercial SC cells by using these electrolytes (Fig. 1(a)). The connection between SC cell and measurement cables with minimized contact resistance, and our test protocols are shown in Fig. 1(b) and (c), respectively. Charge–discharge tests were performed for 10 cycles at each temperature, $+20$, -20, -40 and -55 °C, with constant current of 3 A from 0 to 2.5 V controlled by Arbin (Arbin Instrument). In advance of the measurements, SC cells were stored for 6 h at each temperature in a controlled climatic chamber. After every 10 cycles, cell impedance has been measured at OCV with amplitude of 10 mV from 10 m to 100 kHz controlled by Zahner impedance spectrometer. Floating tests have been performed on the same Batscap SC cells at 2.5 and 2.7 V controlled by VMP3 (BioLogic), for temperatures between $+50$ and $+60$ °C. The cell impedance was measured at each voltage with amplitude of 10 mV from 10 m to 100 kHz with VMP3, recorded every 24 h during 1 month.

3. Electrochemical characterizations

The measured conductivity data is shown in Fig. 2. The conductivity of the AN-based electrolyte in the studied T range is similar to those reported in the literature [3], with an expected decrease of conductivity with decreasing T. Since the temperature of -55 °C was below the freezing point of the AN electrolyte, it was impossible to measure conductivity. The conductivity for MA-
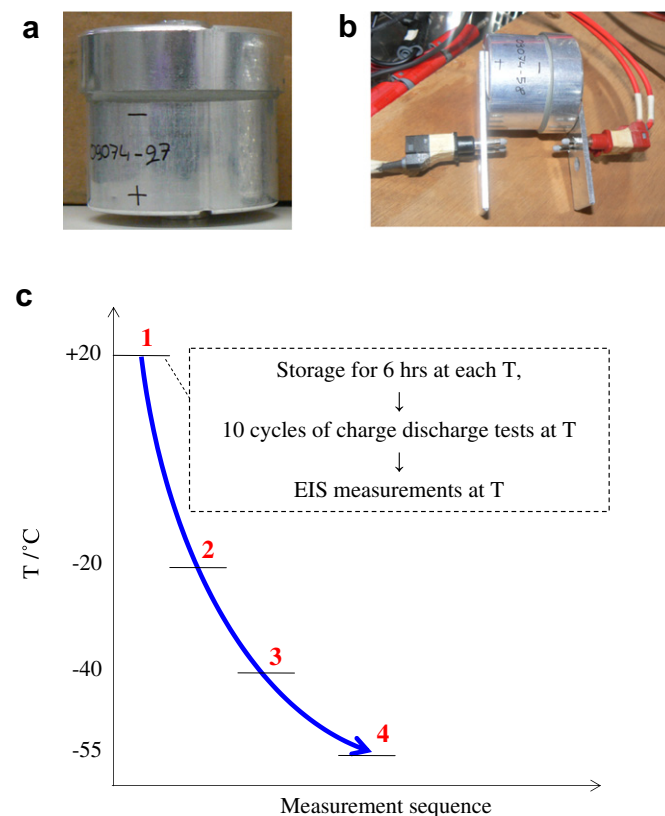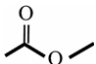
Fig. 1. Images of (a) assembled 600 F 12W SC cell and (b) connected SC cell with cables and (c) our test protocol.

Table 1
Physical properties of acetonitrile and methyl acetate [3].

	Acetonitrile CH$_3$C≡N	Methyl acetate
T_m/°C	-43.8	-98.0
T_b/°C	81.6	56.9
η/cP	0.341	0.364
ε/–	35.9	6.68

Fig. 2. Electrolyte conductivity vs. temperature for the three electrolytes studied, 1 M TEABF$_4$ in ($\bigcirc$) AN, ($\triangle$) AN + MA (75:25) and ($\square$) AN + MA (67:33).

mixed electrolytes was lower than those for the AN electrolyte. The value decreased with an increase in volume of MA from 25 to 33 vol.%, due to the lower dielectric constant of MA than AN as shown in Table 1. Unlike the AN electrolyte, MA-mixed electrolytes were still conductive at −55 °C, showing the highest value of 9 mS cm^{-1} for the MA = 25 vol.%. The discharge curves at every 10th cycles for temperatures between −55 and +20 °C were shown in Fig. 3. From −40 to +20 °C, curves for all three electrolytes maintained their linear shapes, showing typical capacitive behavior [3]. At −55 °C, the difference in the shape became clear with and without MA. For the AN electrolyte, no charge discharge response was observed as shown in Fig. 3(a). The vertical voltage drop is indicative of a large resistance for AN electrolyte. This result clearly shows that AN electrolyte doesn't work at −55 °C, which is lower than AN freezing point of −45 °C. MA-mixed electrolytes, however, maintained their linear shape with a slight decrease in their capacity (Fig. 3(b) and (c)). Thus, this result shows that mixing MA with AN decreases the freezing point of electrolyte mixture without any serious degradation of charge-discharge performances which was previously shown [3]. The capacitance calculated from discharge curves is given in Fig. 4. From +20 to −40 °C, the capacitance for three electrolytes remains almost constant. The capacitance for AN electrolyte were slightly superior to those of MA-mixed electrolytes, while 25 vol.% MA mixture showed higher capacitance than 33 vol.%. At −55 °C, as discussed above, AN electrolyte showed no capacitance, while capacitance for 25 and 33 vol.% MA mixtures maintain 95 and 91% of the capacitance at 20 °C.

To investigate the change of the resistance components, electrochemical impedance spectroscopy (EIS) for three electrolytes at different temperatures were measured. For all the data, the connection resistance of cables was subtracted from real part impedance. As shown in Fig. 5(a), EIS spectra for AN electrolyte show typical EIS spectra of SC and remained same shape in the range between −40 and +20 °C [18]. As expected, only the high frequency resistance shifts to higher value while T decreased. At −55 °C, however, the large semi-circle was suddenly observed and the whole resistance increased from 1.8 mΩ to 19 Ω. Appearance of the large semi-circle suggests a large reformation of interface
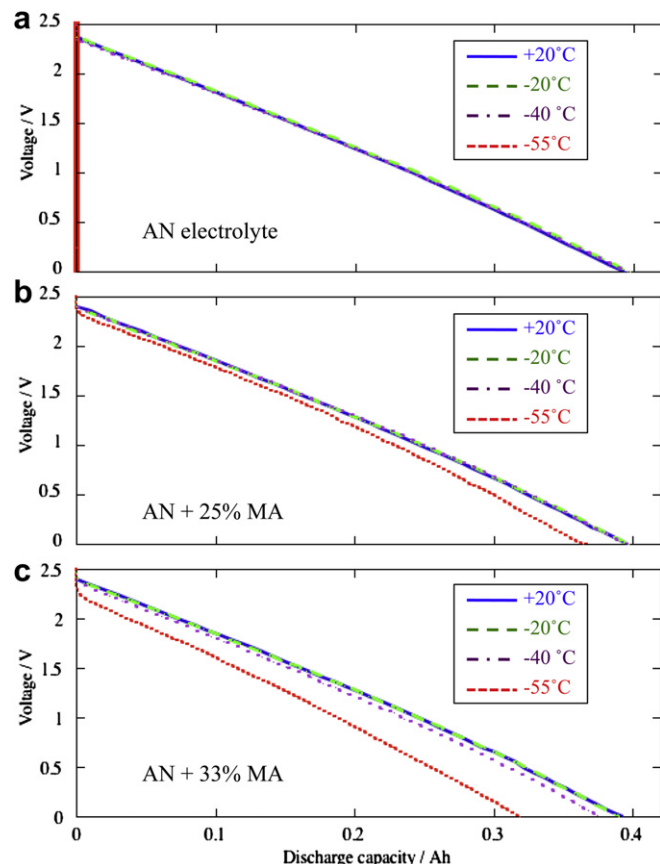

Fig. 3. Discharge curves for 1 M TEABF$_4$ in (a) AN, (b) AN + MA (75:25 in volume) and (c) AN + MA (67:33) at +20, −20, −40 and −55 °C.

between electrolyte and electrode due to the crystallization of AN electrolyte [3]. In comparison, resistance for MA-mixed electrolytes increases with a decrease of temperature from 20 to −55 °C (Fig. 5(b) and (c)). Below −40 °C, even small semi-circle due to the
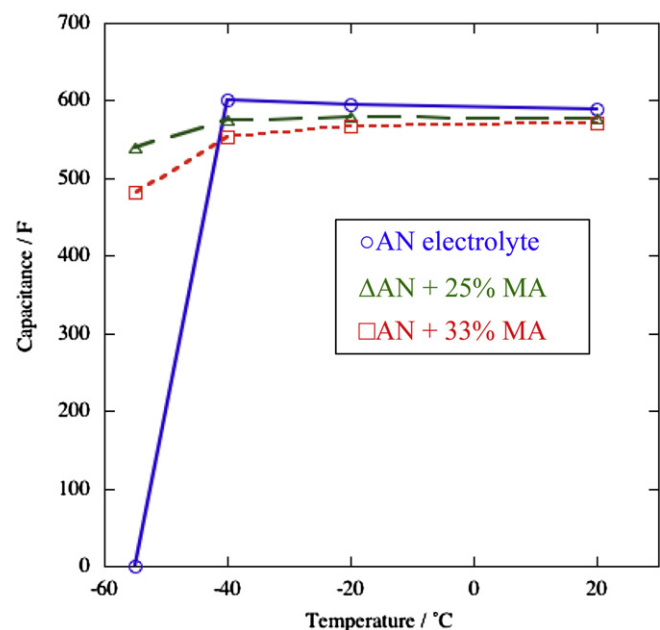
Fig. 4. Evaluated capacitance from discharge curves for 1 M TEABF$_4$ in ($\bigcirc$) AN, ($\triangle$) AN + MA (75:25) and ($\square$) AN + MA (67:33) at +20, −20, −40 and −55 °C.
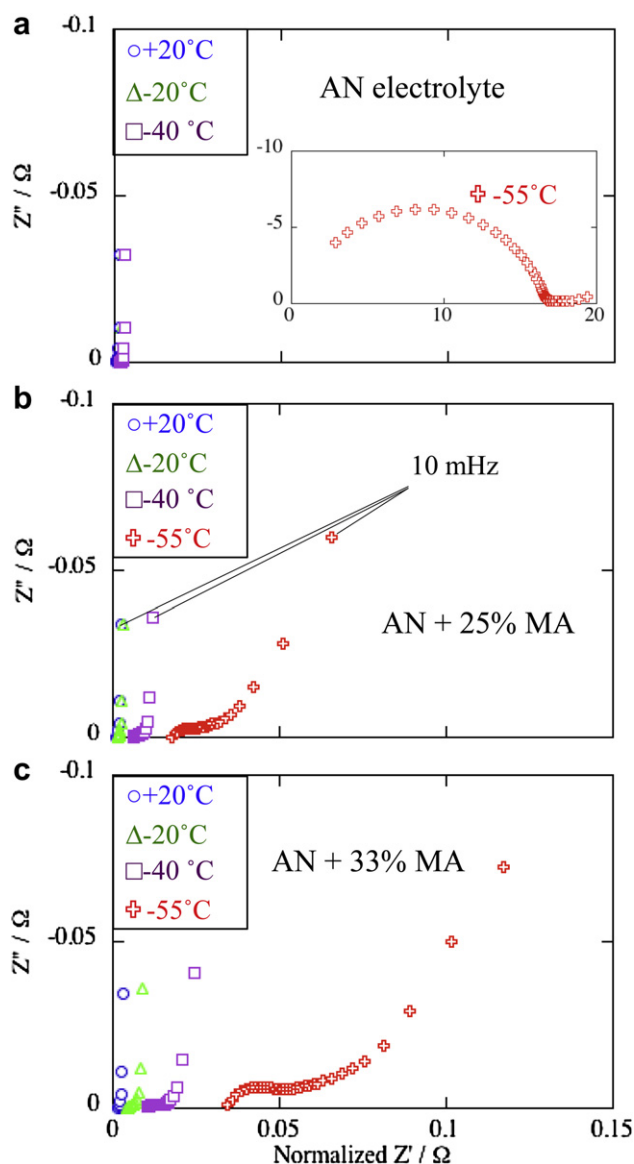
Fig. 5. Niquist plots measured at OCV for 1 M TEABF$_4$ in (a) AN, (b) AN + MA (75:25) and (c) AN + MA (67:33) at +20, −20, −40 and −55 °C. Amplitude was 10 mV and the frequency range was from 10 m to 100 kHz.

Fig. 6. (a) change of resistance at 1 kHz ($R_{@1kHz}$) with temperature and (b) ionic resistance in carbon pores estimated from ESI results for 1 M TEABF$_4$ in (○) AN, (△) AN + MA (75:25) and (□) AN + MA (67:33) at +20, −20, −40 and −55 °C.

modification of the contact between electrode and electrolyte appeared. Unlike results of AN electrolyte, the increase of low frequency resistance at −55 °C for MA-mixed electrolytes remains acceptable with value from 0.07 to 0.11 Ω. Fig. 6(a) shows the change of resistance at 1 kHz ($R_{@1kHz}$) with temperature, except large value of $R_{@1kHz}$ for AN electrolyte at −55 °C (16.4 Ω). From 20 to −55 °C, $R_{@1kHz}$ for all 3 electrolytes increases with a decrease in temperature. Furthermore, we evaluated ionic resistance (R_{ionic}) in porous carbons from EIS spectra and results were plotted in Fig. 6(b). As shown in inlet of Fig. 6(b), R_{ionic} was calculated by subtracting R_{start} to R_{end}, and this allowed us to discuss the pure resistance increase for different electrolyte [19]. At +20 °C, the order of R_{ionic} was 0.6 mΩ for (c) MA = 33 vol.% > 0.4 mΩ for (b) MA = 25 vol.% > 0.2 mΩ for (a) AN electrolyte. Higher R_{ionic} for the MA mixtures is due to a decrease in ionic conductivity by mixing MA as shown in Fig. 2. The order was same until down to −40 °C and the R_{ionic} for (a) increased very slightly from 0.2 to 0.5 m Ω, while that for (b) was from 0.4 to 3.6 mΩ, and that for (c) was from

0.6 to 7 m Ω. This order of R_{ionic} corresponds to the measured conductivity at −40 °C as well. At −55 °C, the R_{ionic} for AN electrolyte was not evaluable due to the large EIS spectra change, while the value was minimized to 36 mΩ for (b) MA = 25 vol.%. This clearly shows that MA = 25 vol.% mixture was superior at −55 °C charge−discharge operation, due to the low resistance of ionic resistance in the carbon pores (Fig. 3).

Floating tests at high temperature at the temperature between 50 and 60 °C for 4 weeks (1 month) were performed with an SC cell composed of 25 vol.% MA-mixed electrolytes, since we were aware of the concern of low boiling point of MA (56.9 °C) compared to that of AN (81.6 °C). Fig. 6(a) shows EIS spectra for the SC cell floated at 2.7 V, 60 °C during 1 month. No obvious change can be seen in the shape of EIS spectra. These results clearly show that equivalent series resistance (ESR) of the cell for 25 vol.% MA mixed electrolyte remained constant even under severe high temperature 60 °C and high voltage 2.7 V. The capacitance C of floated SC were evaluated from the following equation; $C = -1/(2\pi f Z'')$, where f is the frequency and Z'' is the corresponding imaginary impedance. Obtained capacitance for difference temperature and voltage were plotted in Fig. 7(b). After 1 week, slight decrease in capacitance was observed from the initial capacitance for every 3 conditions. Even though there is difference in capacitance for 3 conditions, the values of capacitance retention (=Capacitance/Capacitance at 0 week) are same. After 2 weeks their capacitance remained almost stable until the end of floating tests. These results show that the SC 600 F cells 25 vol.% mixing of MA endured during the 4 weeks floating tests at high temperatures.
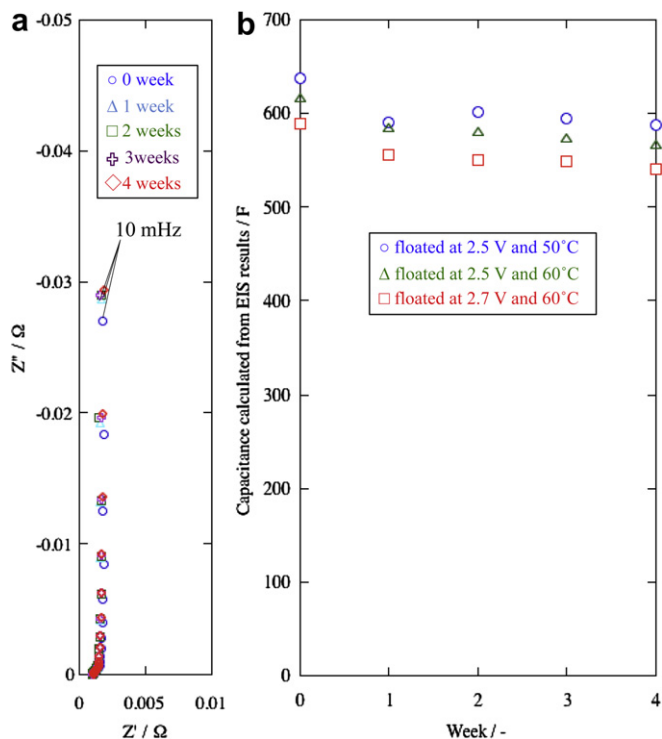
Fig. 7. (a) Niquist plots for 1 M TEABF$_4$ in AN + MA (75:25) at 2.7 V and +60 °C for 1 month. (b) Evaluated capacitance for 1 M TEABF$_4$ in AN + MA (75:25) at (◯) 2.5 V and 50 °C, (△) 2.5 V and 60 °C, and (☐) 2.7 V and +60 °C for 1 month.

4. Conclusions

Mixing MA into conventional AN-based electrolyte successfully enlarged the low temperature operation range of commercial 600F SC cells from −40 to −55 °C. After the modification of MA mixing composition, 25 vol.% of MA mixture was slightly superior to the 33 vol.% MA mixture. These 25 vol.% MA mixtures can operate at high temperature as well, exemplified by floating tests at 2.7 V and +60 °C for 1 month.

References

[1] O. Langlois, E. Foch, X. Roboam, H. Piquet, J3eA 4 (2005) 1.
[2] A. Griffo, J. Wang, Elect. Power Syst. Res. 82 (2012) 59.
[3] E.J. Brandon, C. William, M.C. Smart, L.D. Whitcanack, A. Gary, A. Plett, J. Power Sources 170 (2007) 225.
[4] P. Simon, Y. Gogotsi, Nat. Mater. 7 (2008) 845.
[5] J.R. Miller, P. Simon, Science 321 (2008) 651.
[6] http://www.citroen.fr/technologie-ehdi/#/technologie-ehdi/ (accessed 06.04.12).
[7] http://www.peugeot.com.au/media/deliacms/media/19/1935-4fbb65.pdf (accessed 06.04.12).
[8] L.L. Zhang, X.S. Zhao, Chem. Soc. Rev. 38 (2009) 2520.
[9] Q. Cheng, J. Tang, J. Ma, N. Shinya, L.C. Qin, Phys. Chem. Chem. Phys. 13 (2011) 17615.
[10] V. Presser, M. Heon, Y. Gogotsi, Adv. Funct. Mater. 21 (2011) 810.
[11] M. Arulepp, L. Permann, J. Leis, A. Perkson, K. Rumma, A. Jänes, E. Lust, J. Power Sources 133 (2004) 320.
[12] A. Jänes, E. Lust, Electrochem. Commun. 7 (2005) 510.
[13] A. Jänes, E. Lust, J. Electroanal. Chem. 588 (2006) 285.
[14] E.J. Brandon, M.C. Smart, W. West, Nasa Tech. Briefs 32 (2008) 32.
[15] E.J. Brandon, M.C. Smart, C. William, Nasa Tech. Briefs 34 (2011) 44.
[16] Y. Korenblit, A. Kajdos, W.C. West, M.C. Smart, E.J. Brandon, A. Kvit, J. Jagiello, G. Yushin, Adv. Funct. Mater. 22 (2012) 1655.
[17] R. Lin, P.L. Taberna, S. Fantini, V. Presser, C.R. Perez, F. Malbosc, N.L. Rupesinghe, K.B.K. Teo, Y. Gogotsi, P. Simon, J. Phys. Chem. Lett. 2 (2011) 2396.
[18] A. Balducci, R. Dugas, P.L. Taberna, P. Simon, D. Ple, M. Mastragostino, S. Pass, J. Power Sources 165 (2007) 922.
[19] B.E. Conway, Electrochemical Supercapacitors: Scientific Fundamentals and Technological Applications, Kluwer-Plenum, New York, 1999.